Supplementary Material to manuscript:
Evaluation of a socio-hydrological water resource model for drought management in groundwater-rich areas

Doris E. Wendt[1], Gemma Coxon[1], Saskia Salwey [3], and Francesca Pianosi[2]

[1]School of Geographical Sciences, University of Bristol, Bristol, United Kingdom of Great Britain
[2]School of Civil, Aerospace and Design Engineering, University of Bristol, Bristol, United Kingdom of Great Britain
[3]Department of Physical Geography, Faculty of Geosciences, Utrecht University, Utrecht, The Netherlands

Correspondence: Doris E. Wendt (doris.wendt@bristol.ac.uk)

S1 Overview surface water and groundwater modelling GB

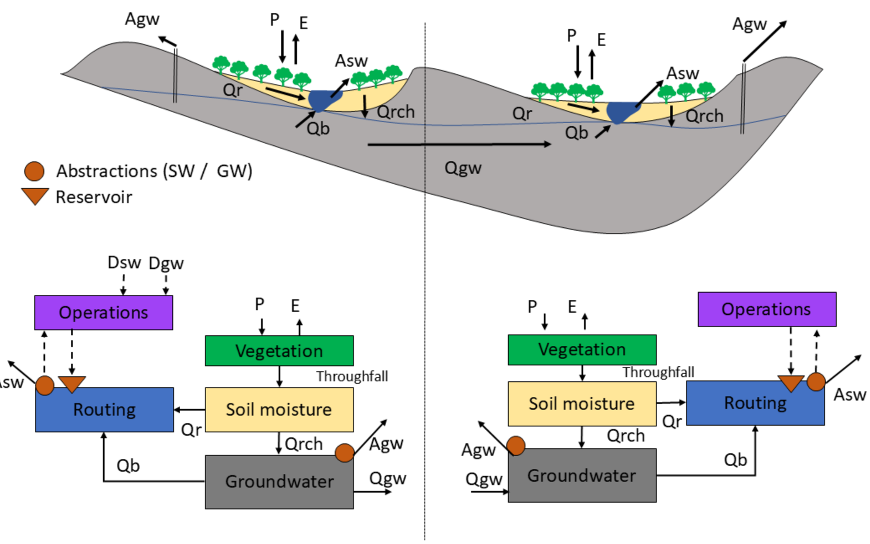

Figure S1. Schematic cross-section of atmospheric, surface and sub-surface fluxes with water management interventions and operations in an groundwater-rich area. Shown fluxes include precipitation (P), evaporation (E), runoff (Qr), baseflow (Qb), groundwater recharge (Qrch), lateral groundwater flow (Qgw), demand for surface water (Dsw) and groundwater (Dgw) and abstractions for surface water (Asw) and groundwater (Agw).

Table S1. Overview of 10 primarily *surface water* focused and groundwater models applied in the UK. Models are sorted based by publication year. Spatial representation is simplified to gridded, lumped and semi-distributed models (column 3). Model fluxes in the represented model components (following from Figure S1 below) are presented in columns 4-9 (operations split for reservoir operations and abstractions) using the abbreviations of Figure S1 with abbreviations for input in model component and black for output. Fluxes representing water management practices or operations are shown in **bold**. Primary model output (flux or state variable), calibration parameters are indicated. Please note that these parameters need to be compatible with the spatial representation of the model. Access to model code is in the last column.

Model name & reference			**Fluxes in physical model components**				**Operations**		**Primary model output**		
	Year	Spatial repres.	Vegetation	Soil moisture	Routing	subsurface	Reservoir	Asw, Agw	Flux / state variable	Calibr. param.	Access to model code
Grid-to-Grid (Bell et al., 2007)	2007	Gridded	-	P, E Qr, Qrch	-	Qrch Qb	-	-	Qb	5	?
AquiMod (Mackay et al., 2014)	2014	Lumped	-	P, E Qf, Qrch	-	Qrch Qb + Qgw	-	-	GWL	13	Under licence
GR4/GR6J (Coron et al., 2017)	2017	Lumped		P, E Qr, Qrch	-	Qrch Qb	-	-	Qb	4	CRAN
SHETRAN-GB (Lewis et al., 2018)	2018	Gridded	P, E	Qr, Qrch	Qr, **Asw** Qb	Qrch,**Agw** Qgw	-	-	Qb, Qgw, GWL	35	email
DECIPHeR (Coxon et al., 2019)	2019	Semi-distr.	P, E	Qr, Qrch	Qr,**Asw** Qb	-	-	-	Qb	7	Github
JULES-GBR (Batelis et al., 2020)	2019	Gridded	P, E	Qr, Qrch	-	Qrch Qb	-	-	Qr, Qb	112	?
SHETRAN-RES (Hughes et al., 2021)	2021	Gridded	P, E	Qf, Qrch	Qr, Qrch, **Asw** Qb, **Res**	-	**Asw** **Res**	-	Qb, Res	46	Github
2D GW model (Rahman et al., 2023)	2023	Gridded	P, E	Qrch	-	Qrch Qgw	-	-	Qgw, GWL	2	Github
BGWM (Bianchi et al., 2024)	2024	Gridded	-	-	-	Qrch Qgw	-	QAgw	Qb, Qgw, GWL	4	licenced
Socio-hydrological model (Wendt et al., 2021)	2021	Lumped	-	P, E Qr, Qrch	-	Qrch Qb + Qgw	**Dsw**, **Res**	**Dsw**,**Dgw** **Asw**, **Agw**	Qb, GWL Asw, Agw	13	Github [2025]

S2 SHOWER modelling equations

The presented model in this paper, SHOWER, is based on the socio-hydrological model of Wendt et al. (2021). This section explains the working of SHOWER in detail with all equations for the lumped modelling of soil moisture, one of the three groundwater modules, a surface water reservoir and the water demand components for both anthropogenic and environmental water demand (Figure 1 in the main manuscript). We also highlight where SHOWER is modified from the socio-hydrological model in (Wendt et al., 2021) in the last 3 paragraphs.

The core of the main model components (soil moisture balance, groundwater modules and water demand module) is similar to the original model. SHOWER is using a daily time step and is ultimately driven by climate data, i.e. precipitation (P in mm d^{-1}) and potential evaporation (ETp_t in mm d^{-1}). Actual evaporation (ETa_t in mm d^{-1}) is calculated based on the amount of soil moisture at a time (SS_t in mm d^{-1}) in Equation S1 following the original soil moisture module in Van Lanen et al. (2013). ETa_t was equal to ETp_t when SS_t is between field capacity (SS_{FC}) and critical soil moisture content (SS_{CR}). Actual evaporation was reduced for drier soils and taken as zero when the soil was below wilting point (SS_{WP}).

$$ETa_t = \begin{cases} ETp_t & \text{if } SS_t \geq SS_{FC} \\ ETp_t * \frac{SS_t - SS_{CR}}{SS_{FC} - SS_{CR}} & \text{if } SS_t < SS_{CR} \\ 0 & \text{if } SS_t < SS_{WP} \end{cases} \tag{S1}$$

Stored water in SHOWER's soil moisture model component can be discharged as runoff (Qr_t in mm d^{-1}), when the soil is saturated (above field capacity, see Equation S2). For this, SHOWER depends quite heavily on set soil characteristics that determine the saturation and total storage. Stored soil moisture can also be passed on as recharge (Rch_t in mm d^{-1}). Again, this process is based on soil characteristics such as the daily soil moisture content, the retention shape parameter (b) and unsaturated hydraulic conductivity (Kfc) (See Equation S3, Van Lanen et al. (2013)). All together, these components define the complete soil moisture balance, which drives both surface water and groundwater flow and storage (Equation S4).

$$Qr_t = \begin{cases} SS_t - SS_{FC} & \text{if } SS_t > SS_{FC} \\ 0 & \text{if } SS_t \leq SS_{FC} \end{cases} \tag{S2}$$

$$Rch_t = \begin{cases} 0 & \text{if } SS_t \geq SS_{FC} \\ \left(\frac{SS_t - SS_{CR}}{SS_{FC} - SS_{CR}}\right)^b k_{FC} & \text{if } SS_{CR} < SS_t < SS_{FC} \\ 0 & \text{if } SS_t \leq SS_{CR} \end{cases} \tag{S3}$$

$$SS_t = SS_{t-1} + P_t - ETa_t - Qr_t - Rch_t \tag{S4}$$

The total available water for anthropogenic water demand (ADem in mm d^{-1})) is derived from the average annual runoff and recharge. Following a range of different water resource management plans in the UK, allocated ADem is defined as a fraction (f_{dem}) of the long-term average of annual runoff and groundwater recharge that is divided equally over the days of the year (Equation S5). f_{dem} is defined by the proportional water use as reported by drinking water companies, see Wendt et al. (2021) for more details. The water withdrawn from groundwater stores and the reservoir can change depending on which (user-input) management scenario is at play. Both groundwater abstractions (Agw in mm d^{-1}) and/or surface water abstractions (Asw in mm d^{-1}) are in place, but these can be 'turned off' conditionally or permanently. One modelled condition to reduce water demand is related to the ecological minimum flow (meeting environmental water demand) that reduces when baseflow is below the (Qb_{eco}) threshold.

When water demand exceeds stored water, two (similar) conditions are in place. When reservoir storage declines, additional (unlimited) surface water (Qimp in mm d^{-1}) is imported in the baseline scenario. In current drought management scenarios, reservoir storage is refilled when storage levels are below 25% of the reservoir levels, representing the regular water transfers as part of the drought management strategies (see Table 1 in (Wendt et al., 2021); also described in Dobson et al. 2020). For groundwater storage, additional storage (Gs_{lat} in mm d^{-1}) can be imported at any time in a similar manner to imported surface water. This might be referred as incoming lateral groundwater flow, as groundwater aquifer storage can exceed the surface water boundaries (Allen et al., 1997; de Graaf et al., 2019).

$$ADem = \frac{f_{dem} * (\overline{\sum Qr} + \overline{\sum Rch})}{365} \tag{S5}$$

Surface water, either runoff or/and baseflow, in the model can be stored in a reservoir (Figure **??**; see also Equation S6). In the upstream reservoir setup, runoff (Qr) and baseflow (Qb in mm d^{-1}) make up the majority of the stored water. From baseflow, we subtract ecological minimum flow prior to adding this to the reservoir (QbRes) see Equation S8. The remaining stored water (Qr and QbRes in mm) are used to meet surface water demand, which is 44.6% of allocated water in the baseline and variable in the drought management scenarios (Wendt et al., 2021). Maximum reservoir storage (Rcap) is a model parameter expressed as a percentage of the annual average precipitation. When the reservoir capacity is exceeded, excess reservoir storage (Qrel in mm d^{-1}) leaves SHOWER, which is essentially overflow of a reservoir and is not used to meet surface water demand (see Equation S7).

$$Res_t = \begin{cases} Res_{t-1} + Qr_{t-1} + QbRes_{t-1} + Qimp_{t-1} - Dsw - Qrel_{t-1} & \text{if } Res_t \leq Rcap \\ Res_{t-1} - Rcap - Dsw - Qout_{t-1} & \text{if } Res_t > Rcap \end{cases} \tag{S6}$$

where:

$$Qrel_t = max(0, Rcap - Res_t) \tag{S7}$$

$$QbRes_t = max(0, Qb_t - Qeco) \tag{S8}$$

Groundwater, sustained by daily recharge, is modelled using a groundwater module of choice, as there are three parallel options setup in SHOWER. In either of these modules, recharge is either stored (Gs in mm d^{-1}) or further discharged as baseflow. The amount of baseflow depends on the specific groundwater storage parameter(s) (s in d^{-1}) in each groundwater module (Stoelzle et al., 2015). Each model has their own storage-outflow parameters (s in d^{-1} in Table S2). Ranges for these parameters are based on average characteristics found in English karstic, porous, and fractured aquifers (Allen et al., 1997) and include the tested parameters ranges by Stoelzle et al. (2015).

The first module refers to generally large groundwater availability with non-linear groundwater outflow conditions, as typically found in karstic groundwater systems (Stoelzle et al., 2015; Hartmann et al., 2015). Baseflow release is modelled by a non-linear power law (Equation S9) in which B is given a range from highly turbulent flow (0.3) to linear flow (1), as one might find in unconfined karstic aquifers (Wittenberg, 2003). The second module has a lower groundwater storage but more regular, primarily linear, baseflow release with a small leakage component (Equation S10, as may be found in porous aquifers (Allen et al., 1997; Shepley et al., 2008). The leakage component (7-12%) is based on the tested range by Stoelzle et al. (2015) for this modelling setup. The third module represents relatively small groundwater storage, as may be found in shallow or weathered fractured aquifers (Allen et al., 1997; Stoelzle et al., 2015). This aquifer typology is modelled by two parallel linear storage reservoirs (S11 referring to weathered, fractured aquifers with variable storage-outflow release (Stoelzle et al., 2015; Allen et al., 1997). These two storage reservoirs are treated equal in receiving recharge and abstracting water to meet the water demand.

$$\text{Large groundwater storage system} = \begin{cases} Qb_t = sGS_t^B \\ GS_t = GS_{t-1} + Rch_t - Qb_t - Agw_t \end{cases} \tag{S9}$$

$$\text{Medium groundwater storage system} = \begin{cases} Qb_t = sGS_t + DRch_t \\ GS_t = GS_{t-1} + (1-D)Rch_t - Qb_t - Agw_t \end{cases} \tag{S10}$$

$$\text{Small groundwater storage system} = \begin{cases} Qb_t = s_1GS1_t + s_2GS2_t \\ GS1_t = GS1_{t-1} + \frac{1}{2}Rch_t - s_1GS1_t - \frac{1}{2}Agw_t \\ GS2_t = GS2_{t-1} + \frac{1}{2}Rch_t - s_2GS2_t - \frac{1}{2}Agw_t \end{cases} \tag{S11}$$

Table S2. Groundwater storage-outflow s values (in d^{-1}) for the three groundwater options in the groundwater module. The first row shows s values used by Stoelzle et al. (2015), the second row shows representative s values for England based on Allen et al. (1997), and the third row presents the modelled (mean) s values for the three groundwater options in Equations S9-S11. In the sensitivity analysis, a range of s values was calculated (last row). For the low storage system, only s_1 was changed in the sensitivity analysis. The response time (in days) is shown for the modelled s values in parenthesis.

	Large storage system (s in d^{-1})	**Medium storage system (s in d^{-1})**	**Small storage system (s in d^{-1})**
Optimal s values by Stoelzle et al. (2015)	0.008-0.025	0.001-0.01	s_1 : 0.004-0.011 s_2 : 0.05-0.25
Mean English s values by Allen et al. (1997)	0.009-0.04	0.0008-0.004	0.002-0.02
Modelled s values	0.02 (50 days)	0.004 (250 days)	s_1 : 0.005 (200 days) s_2 : 0.1 (10 days)
Alternative s values	0.01 (100 days) 0.0133 (75 days) 0.03 (33 days)	0.001 (1000 days) 0.002 (500 days) 0.01 (100 days)	0.002 (500 days) 0.00285 (350 days) 0.01 (100 days)

S3 Modifications from socio-hydrological modelling by Wendt et al. (2021)

Modifications from Wendt et al. (2021) in SHOWER followed from initial findings running the Global Sensitivity Analysis and affect mainly the runoff generation. Originally, runoff was generated for both dry and wet conditions, as half of the precipitation was assumed to be bypassing the soil (Van Lanen et al., 2013). However, these conditions are specific to clay rich (agricultural) systems and in desert conditions (Mirus and Loague, 2013), which does not relate to known dominant runoff generation processes in England (Beven, 2012). Consequently, model output in the socio-hydrological model in (Wendt et al., 2021) was dominated by this feature unjustifiably (SI) and therefore, we have modified this in SHOWER as runoff is now only generated for saturated soils. This approach also aligns with other well-received surface models as DeCIPHER (Coxon et al., 2019).

Another modification is the setup of the surface water reservoir, which can be modelled at both upstream and downstream locations. This involved creating an additional (smaller) soil moisture component to the model, which size depends on the upstream contributing area of the reservoir (Salwey et al., 2023). The upstream reservoir releases include the ecological minimum flow (Qeco) in the release flow (Qrel in mm^{-1}; see Equation S12 and S13). These release flows are aimed at sustaining minimum flow conditions that typically vary between 80^{th} and 95^{th} percentile of natural flow conditions (Salwey et al., 2023).

This typical values also aligns with the expected ecological minimum flow by the Environment Agency (Environment Agency, 2020).

$$Res_t = \begin{cases} Res_{t-1} + Qr_{t-1} + Rch_{t-1} + Qimp_{t-1} - Dsw - Qrel_{t-1} & \text{if } Res_t \leq Rcap \\ Res_{t-1} - Rcap - Dsw - Qout_{t-1} & \text{if } Res_t > Rcap \end{cases} \tag{S12}$$

where:

$$Qrel_t = max(Qeco, Rcap - Res_t) \tag{S13}$$

Lastly, in SHOWER the interchangeable groundwater components are linked to primary aquifers in the UK, removing the idealised setting of Wendt et al. (2021). The Chalk aquifer is represented using a large groundwater storage with dominant karstic, non-linear, flow characteristics (Hartmann et al., 2015; Wittenberg, 2003). The Permo-Triassic Sandstone aquifer is modelled using the medium groundwater storage with throughflow in the porous aquifer (Shepley et al., 2008) and lastly, smaller groundwater storage is reflecting the Dinantian Limestone aquifer with predominantly fracture flow releasing groundwater storage (Allen et al., 1997).

S4 Performance of Top 100 simulations ranked by logged NSE

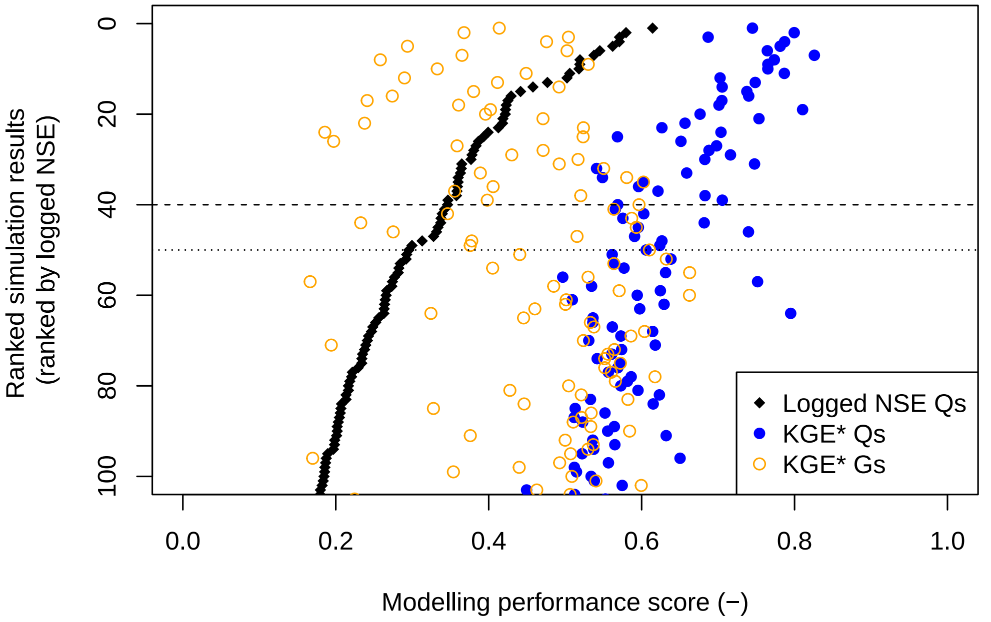

Figure S2. Ranked simulation runs (100) based on logged NSE indicating the step change in logged NSE modelling performance for the Pang catchment around 40-50 runs (see dotted lines).

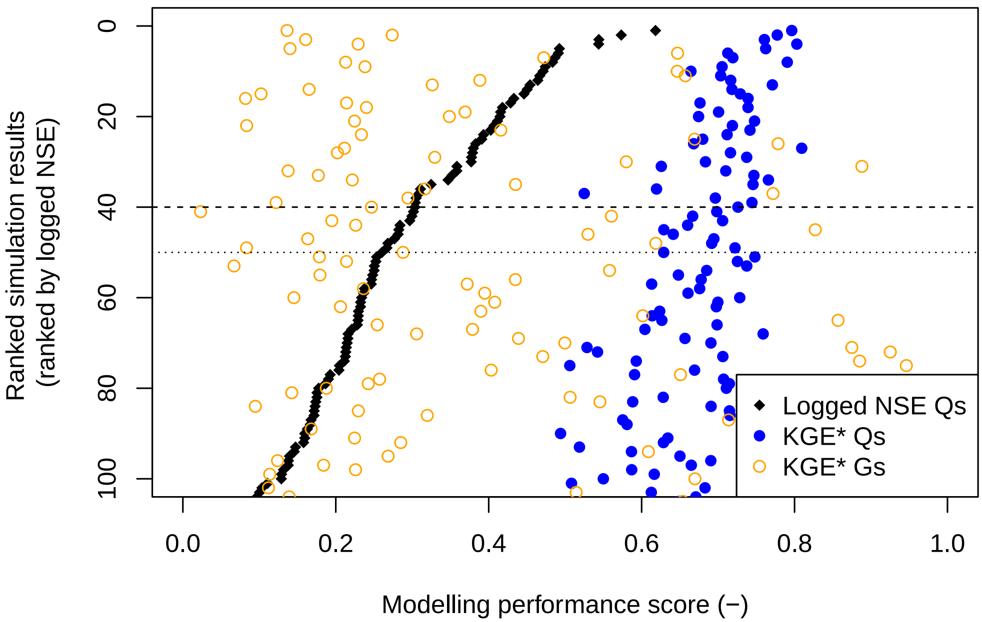

Figure S3. Ranked simulation runs (100) based on logged NSE indicating the step change in logged NSE modelling performance for the Trent catchment around 40-50 runs (see dotted lines).

S5 Overall GSA results for all GW modules

Mean sensitivity of averaged model output for 25 year runs (1990-2014). The colours show the increasing sensitivity of model output to model parameters for the three groundwater modules. Parameter abbreviations on the y-axis match Figure 1 in manuscript. Note that the fractured module has the upstream reservoir modelled, compared to the karstic and porous module that have a downstream reservoir setup.

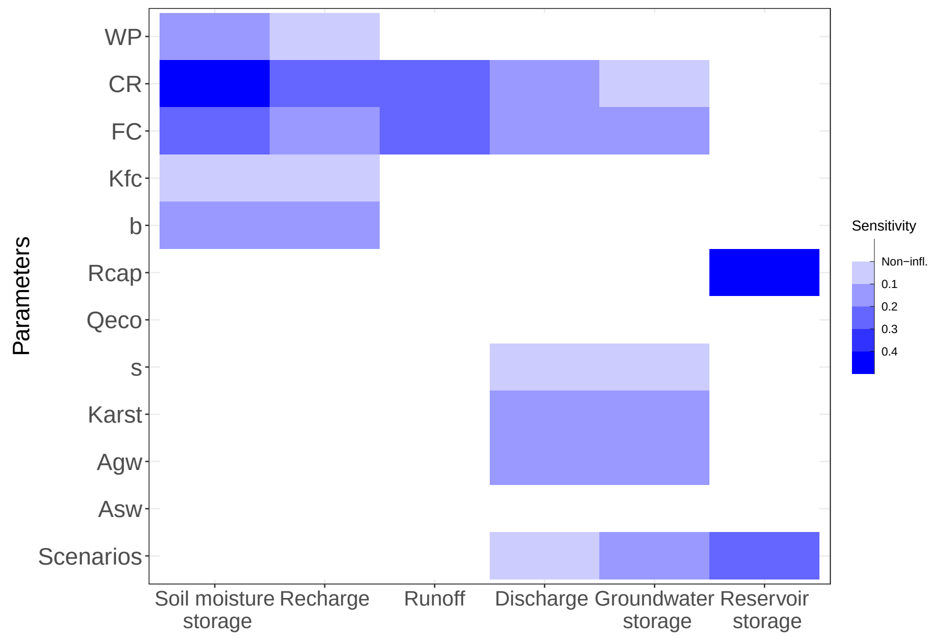

Figure S4. Karstic module

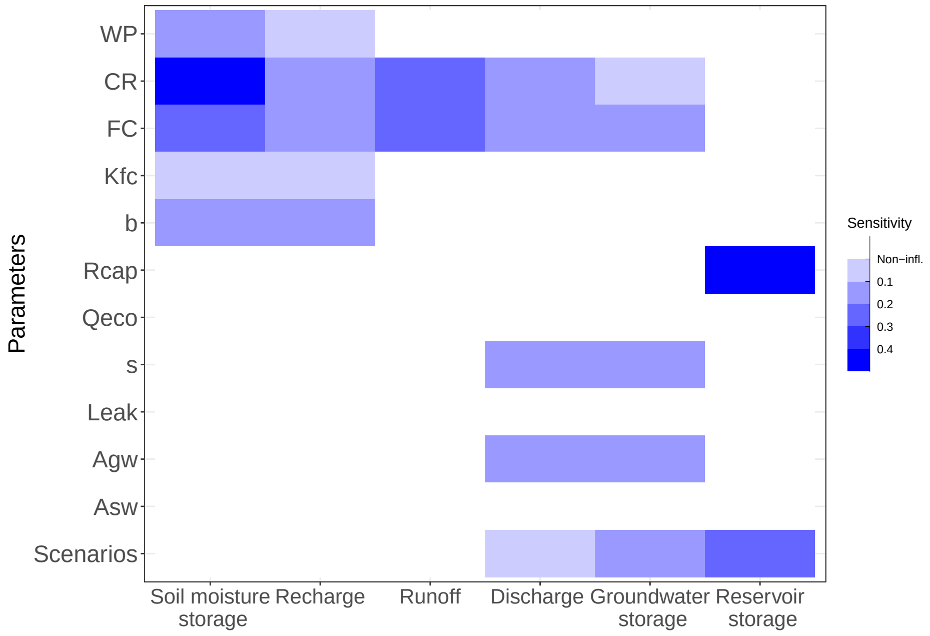

Figure S5. Porous module

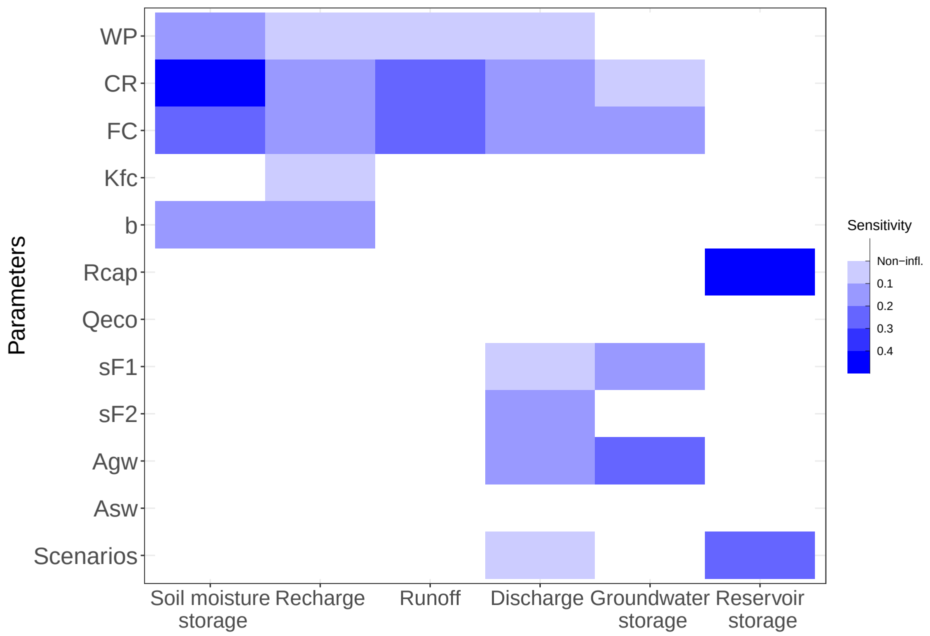

Figure S6. Fracture module

S6 GSA Parameter sensitivity results for porous module

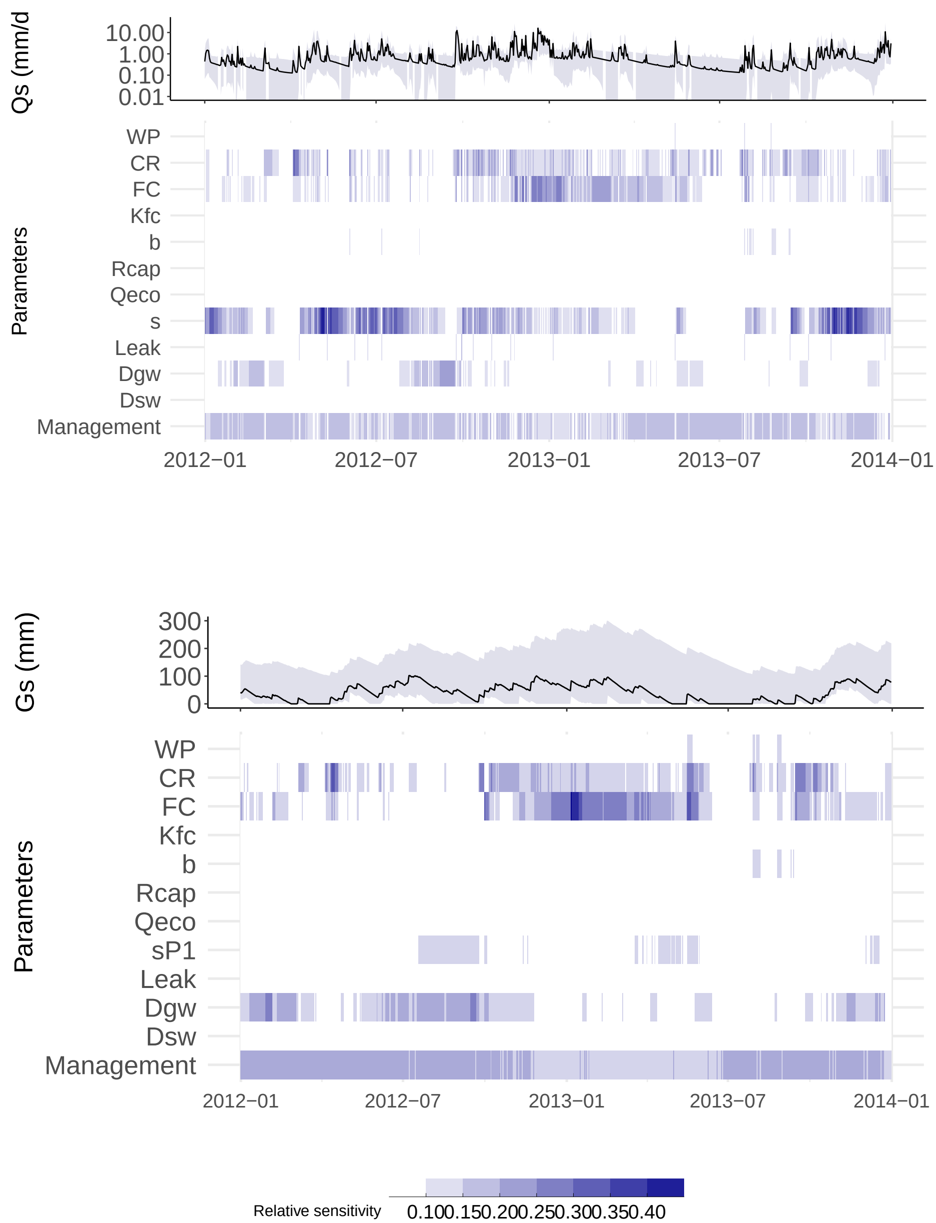

Figure S7. Time varying parameter sensitivity to simulated discharge (above) and groundwater (below), modelled using the porous groundwater-outflow module. Both discharge and groundwater time series are shown using a mean (black solid line) of all 9211 simulations and the 10^{th} and 90^{th} percentile of the two runs.

S7 GSA Parameter sensitivity results for fractured module (groundwater)

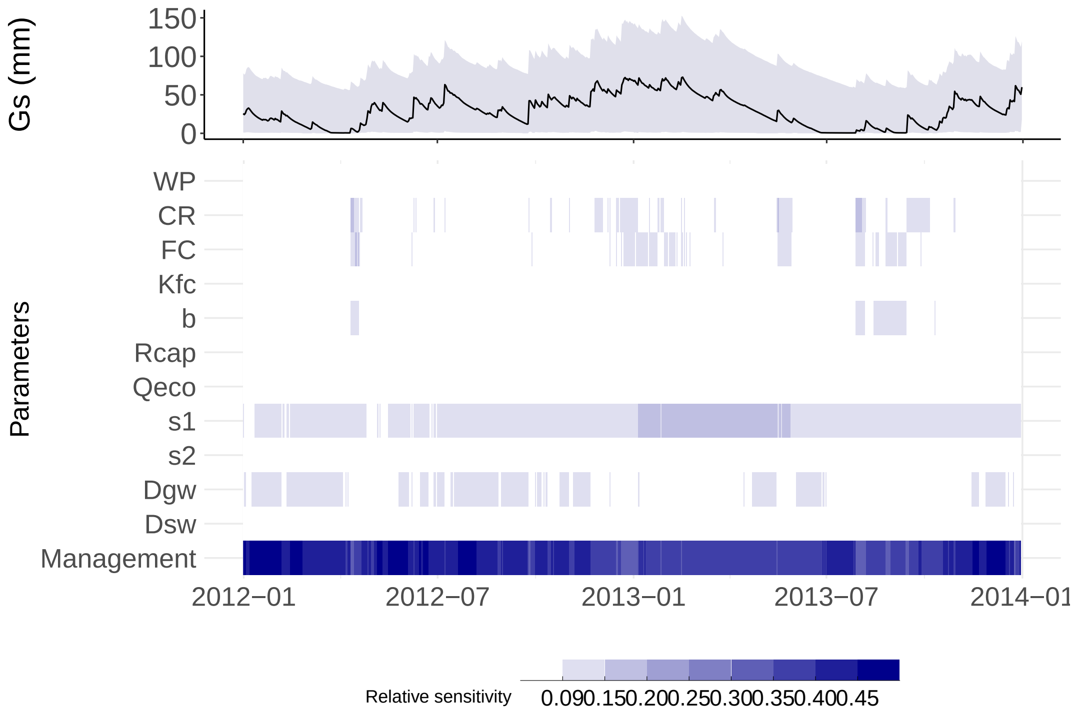

Figure S8. Time varying parameter sensitivity to simulated discharge (above) and groundwater (below), modelled using the fractured groundwater-outflow module. This module has an upstream reservoir modelled, rather than the downstream option applied to both the karstic and porous module. Both discharge and groundwater time series are shown using a mean (black solid line) of all 9211 simulations and the 10^{th} and 90^{th} percentile of the two runs.

S8 Drought characteristics for each management scenario

Mean drought duration (in days; left panel in Figures below), drought deficit (in mm; middle panel) and drought frequency (counted; right panel) shown for all GSA simulations (10K) for all three groundwater modules. Drought characteristics are calculated from baseline - drought management scenario (coloured box plots). A description of the scenarios is in Methods and details can be found in (Wendt et al., 2021).

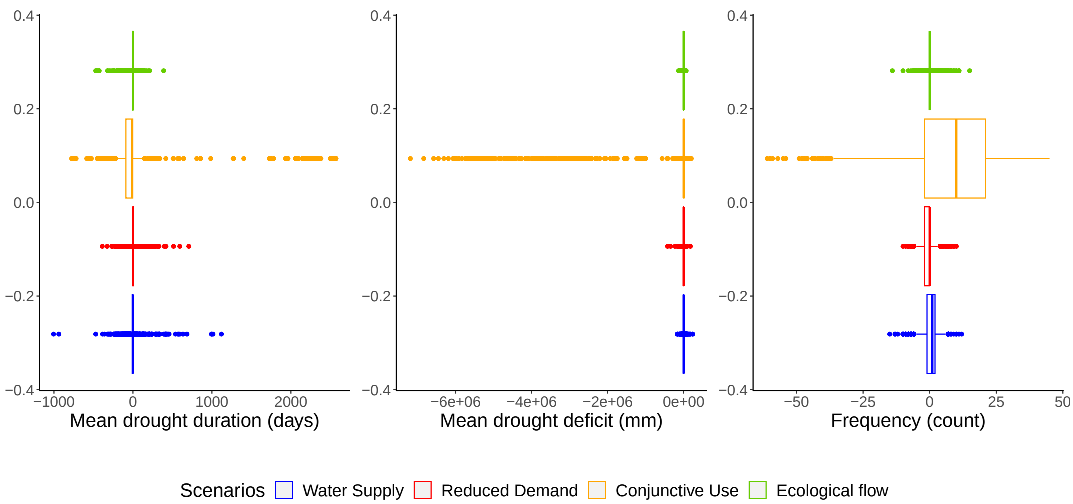

Figure S9. Karstic groundwater module

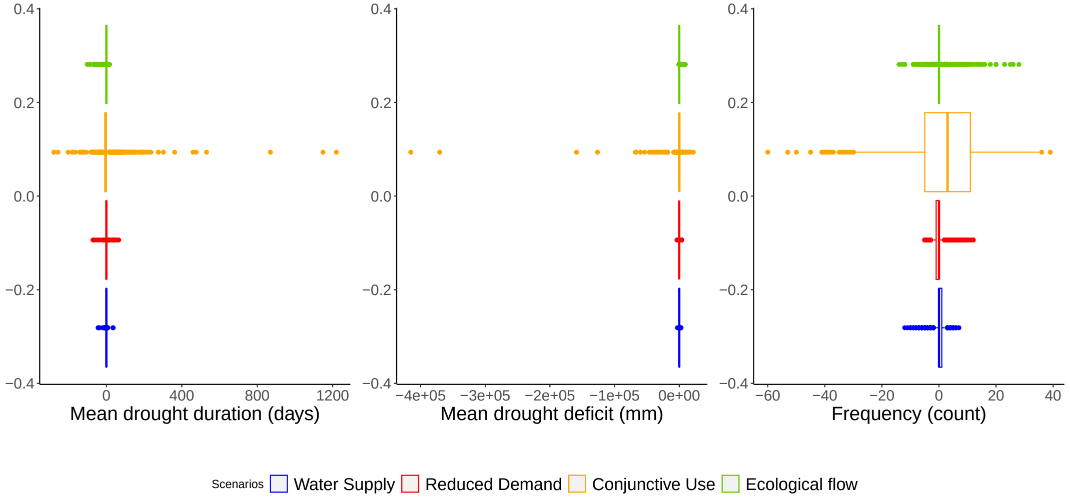

Figure S10. Porous groundwater module

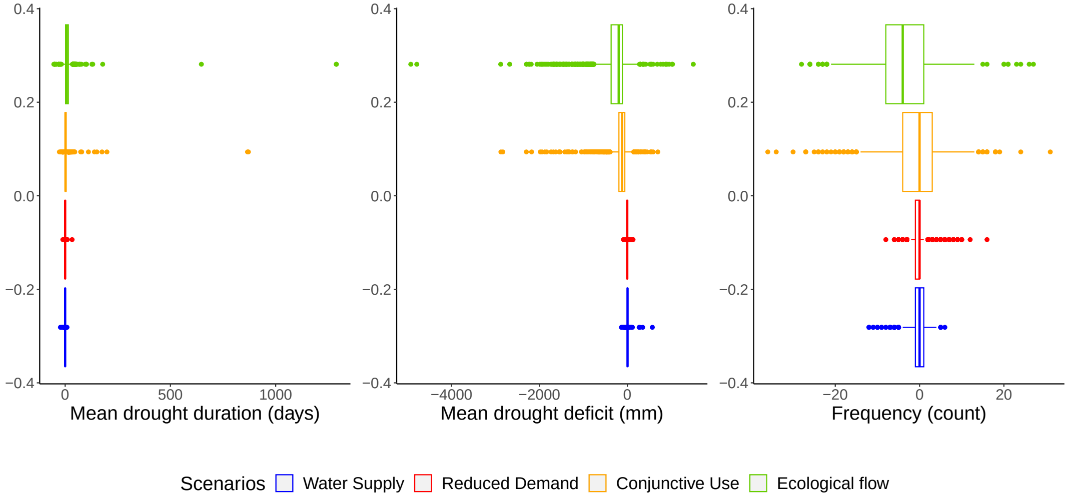

Figure S11. Fractured module

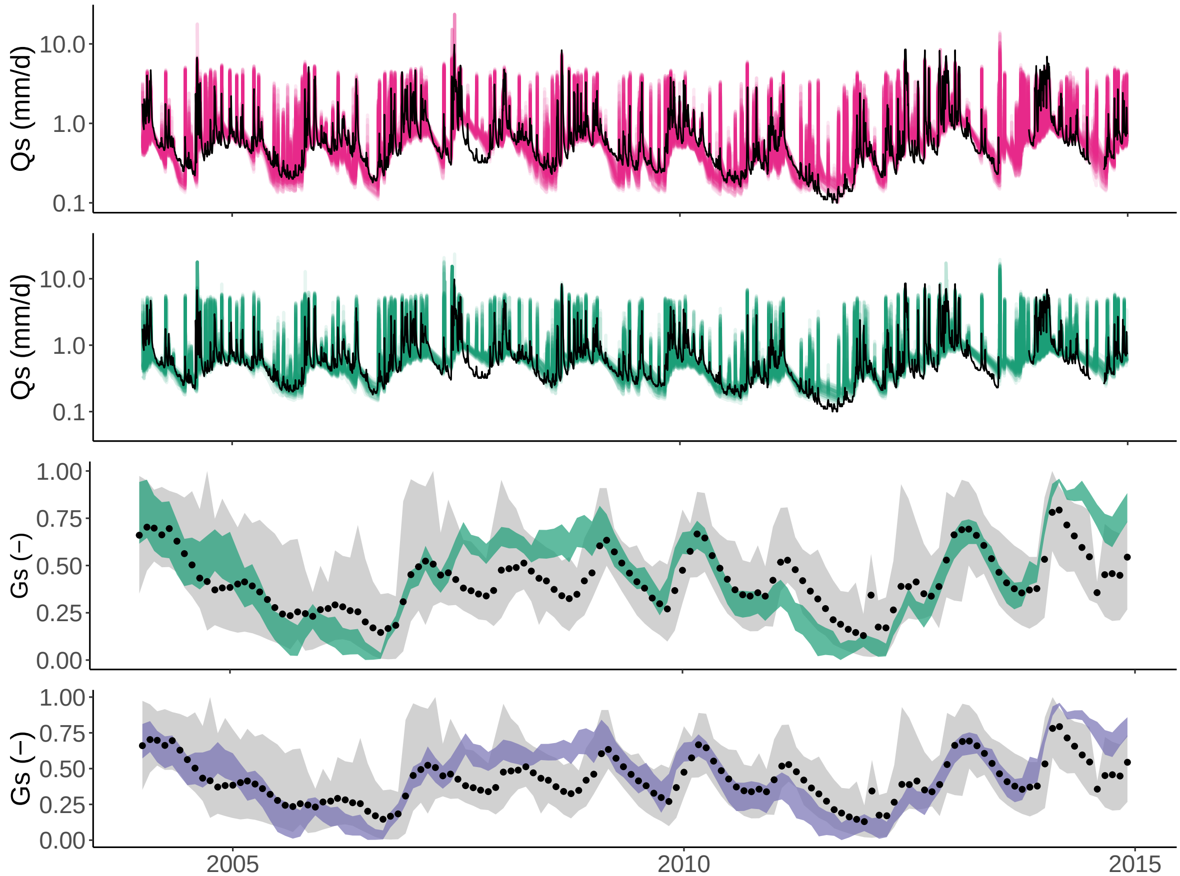

Figure S12. Simulated discharge (Qs (mmd^{-1}) and normalised groundwater storage (Gs (-)) in the **Trent catchment** over the validation period 2004-2014. Top panel shows discharge simulations calibrated on NSE$_{log}$ (in pink) and the middle panels shows discharge calibrated on the 'Best Overall' criteria (in green). The lower two panels show normalised groundwater simulations calibrated on the 'Best Overall' (in green) and KGE-Gs (in purple). Black lines/dots are observations. Note that groundwater level observations are averaged from 4 locations, with the range of variability across the stations in grey.

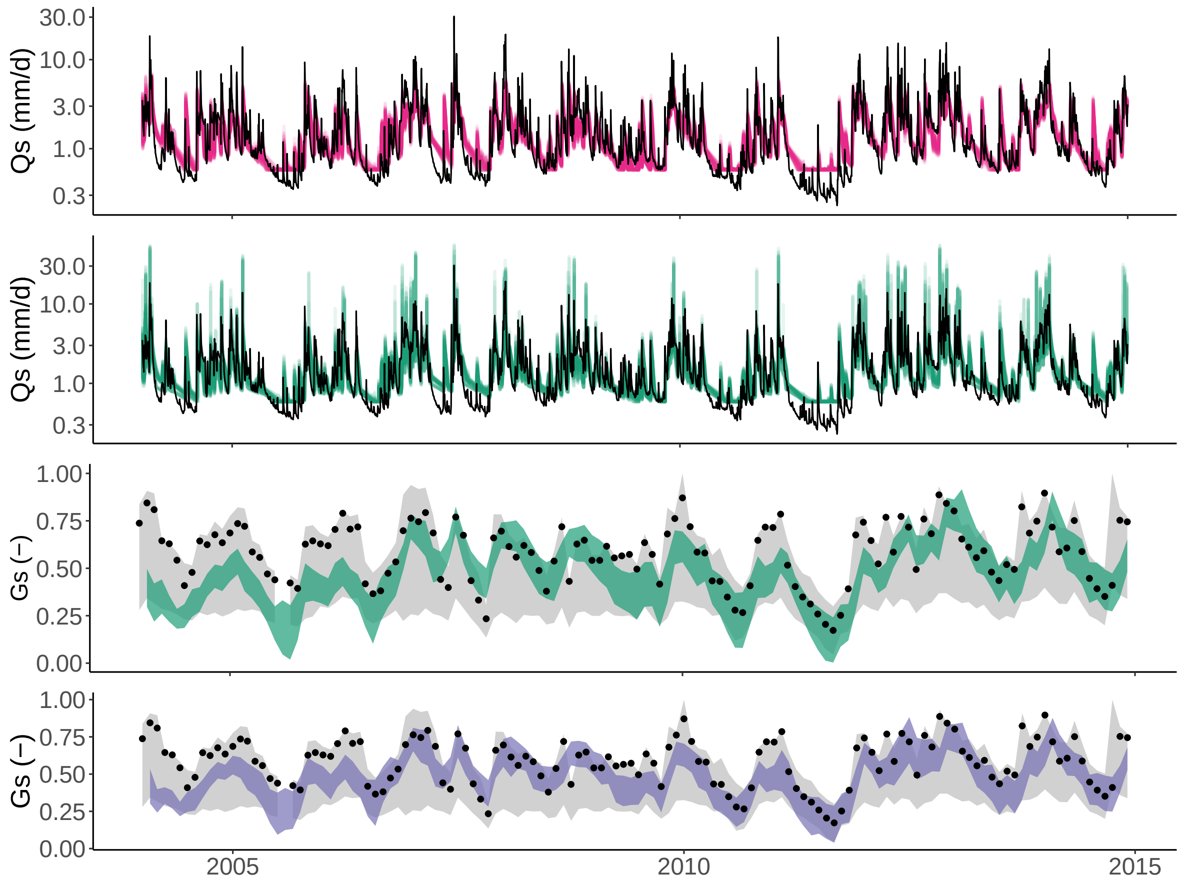

Figure S13. Simulated discharge (Qs (mmd^{-1}) and normalised groundwater storage (Gs (-)) in the **Derwent catchment** over the validation period 2004-2014. Top panel shows discharge simulations calibrated on NSE$_{log}$ (in pink) and the middle panels shows discharge calibrated on the 'Best Overall' criteria (in green). The lower panels show normalised groundwater simulations calibrated on the 'Best Overall' (in green) and KGE-Gs (in purple). Black lines/dots are observations. Note that groundwater level observations are averaged from 5 locations, with the range of variability across the stations in grey.

References

Allen, D., Brewerton, L., Coleby, L., Gibbs, B., Lewis, M., MacDonald, A., Wagstaff, S., and Williams, A.: The physical properties of major aquifers in England and Wales, British Geological Survey (WD/97/034), 1997.

Batelis, S.-C., Rahman, M., Kollet, S., Woods, R., and Rosolem, R.: Towards the representation of groundwater in the Joint UK Land Environment Simulator, Hydrological Processes, 34, 2843–2863, https://doi.org/https://doi.org/10.1002/hyp.13767, 2020.

Bell, V. A., Kay, A. L., Jones, R. G., and Moore, R. J.: Development of a high resolution grid-based river flow model for use with regional climate model output, Hydrology and Earth System Sciences, 11, https://doi.org/10.5194/hess-11-532-2007, 2007.

Beven, K. J.: Rainfall-runoff modelling: the primer, John Wiley & Sons, 2012.

Bianchi, M., , Scheidegger, J., , Hughes, A., , Jackson, C., , Lee, J., , Lewis, M., , Mansour, M., , Newell, A., , O'Dochartaigh, B., , Patton, A., and Dadson, S.: Simulation of national-scale groundwater dynamics in geologically complex aquifer systems: an example from Great Britain, Hydrological Sciences Journal, 69, 572–591, https://doi.org/10.1080/02626667.2024.2320847, 2024.

Coron, L., Thirel, G., Delaigue, O., Perrin, C., and Andréassian, V.: The suite of lumped GR hydrological models in an R package, Environmental Modelling & Software, 94, 166–171, https://doi.org/https://doi.org/10.1016/j.envsoft.2017.05.002, 2017.

Coxon, G., Freer, J., Lane, R., Dunne, T., Knoben, W. J. M., Howden, N. J. K., Quinn, N., Wagener, T., and Woods, R.: DECIPHeR v1: Dynamic fluxEs and ConnectIvity for Predictions of HydRology, Geoscientific Model Development, 12, 2285–2306, https://doi.org/10.5194/gmd-12-2285-2019, 2019.

de Graaf, I. E., Gleeson, T., van Beek, L. R., Sutanudjaja, E. H., and Bierkens, M. F.: Environmental flow limits to global groundwater pumping, Nature, 574, 90–94, 2019.

Dobson, B., Coxon, G., Freer, J., Gavin, H., Mortazavi-Naeini, M., and Hall, J. W.: The Spatial Dynamics of Droughts and Water Scarcity in England and Wales, Water Resources Research, 56, e2020WR027 187, https://doi.org/10.1029/2020WR027187, e2020WR027187 2020WR027187, 2020.

Environment Agency: Meeting our future water needs: a national framework for water resources, techreport, 2020.

Hartmann, A., Gleeson, T., Rosolem, R., Pianosi, F., Wada, Y., and Wagener, T.: A large-scale simulation model to assess karstic groundwater recharge over Europe and the Mediterranean, Geoscientific Model Development, 8, 1729–1746, https://doi.org/10.5194/gmd-8-1729-2015, 2015.

Hughes, D., Birkinshaw, S., and Parkin, G.: A method to include reservoir operations in catchment hydrological models using SHETRAN, Environmental Modelling & Software, 138, 104 980, https://doi.org/https://doi.org/10.1016/j.envsoft.2021.104980, 2021.

Lewis, E., Birkinshaw, S., Kilsby, C., and Fowler, H. J.: Development of a system for automated setup of a physically-based, spatially-distributed hydrological model for catchments in Great Britain, Environmental Modelling & Software, 108, 102 – 110, https://doi.org/https://doi.org/10.1016/j.envsoft.2018.07.006, 2018.

Mackay, J., Jackson, C., and Wang, L.: A lumped conceptual model to simulate groundwater level time-series, Environmental Modelling & Software, 61, 229–245, https://doi.org/https://doi.org/10.1016/j.envsoft.2014.06.003, 2014.

Mirus, B. B. and Loague, K.: How runoff begins (and ends): Characterizing hydrologic response at the catchment scale, Water Resources Research, 49, 2987–3006, https://doi.org/https://doi.org/10.1002/wrcr.20218, 2013.

Rahman, M., Pianosi, F., and Woods, R.: Simulating spatial variability of groundwater table in England and Wales, Hydrological Processes, 37, e14 849, https://doi.org/https://doi.org/10.1002/hyp.14849, 2023.

Salwey, S., Coxon, G., Pianosi, F., Singer, M. B., and Hutton, C.: National-Scale Detection of Reservoir Impacts Through Hydrological Signatures, Water Resources Research, 59, e2022WR033 893, https://doi.org/https://doi.org/10.1029/2022WR033893, e2022WR033893 2022WR033893, 2023.

Shepley, M., Pearson, A., Smith, G., and Banton, C.: The impacts of coal mining subsidence on groundwater resources management of the East Midlands Permo-Triassic Sandstone aquifer, England, Quarterly Journal of Engineering Geology and Hydrogeology, 41, 425–438, https://doi.org/10.1144/1470-9236/07-210, 2008.

Stoelzle, M., Weiler, M., Stahl, K., Morhard, A., and Schuetz, T.: Is there a superior conceptual groundwater model structure for baseflow simulation?, Hydrological Processes, 29, 1301–1313, https://doi.org/10.1002/hyp.10251, 2015.

Van Lanen, H. A. J., Wanders, N., Tallaksen, L. M., and Van Loon, A. F.: Hydrological drought across the world: impact of climate and physical catchment structure, Hydrol. Earth Syst. Sci, 17, 1715–1732, https://doi.org/10.5194/hess-17-1715-2013, 2013.

Wendt, D. E., Bloomfield, J. P., Van Loon, A. F., Garcia, M., Heudorfer, B., Larsen, J., and Hannah, D. M.: Evaluating integrated water management strategies to inform hydrological drought mitigation, Natural Hazards and Earth System Sciences, 21, 3113–3139, https://doi.org/10.5194/nhess-21-3113-2021, 2021.

Wittenberg, H.: Effects of season and man-made changes on baseflow and flow recession: case studies, Hydrological Processes, 17, 2113–2123, https://doi.org/https://doi.org/10.1002/hyp.1324, 2003.